

Characterization of lava tubes using ground penetrating radar at Craters of the Moon National Monument, USA.

Colin R. Rowell, Adam Pidlisecky, James D. Irving*, and Robert J. Ferguson

ABSTRACT

Craters of the Moon National Monument is a Pleistocene to Holocene volcanic field in southern Idaho. It consists of numerous lava flows erupted between 15,000 and 2000 years ago. One of the largest lava flows, called the ‘Blue Dragon’ flow, is approximately 2100 years old and covers an area of 280 km². In many of these larger flows, lava tubes provide an important means of transporting lava underneath the flow over large distances. The goal of this project is to use near-surface geophysical techniques to build images of lava tubes in the sub-surface, and use this information to better understand the mechanisms of lava transport that were active during the eruption.

Ground-penetrating radar (GPR) is a geophysical technique that transmits radio waves into the ground, which are then reflected off of boundaries in the sub-surface. These reflected waves return to the surface to be recorded by the radar device. From these reflections, a 2-dimensional image of the sub-surface can be assembled. This technique was used to image lava tubes at Craters of the Moon National Monument.

GPR data were acquired over known lava tubes in order to assess the usefulness of the method for detecting lava tubes and other lava flow features. A standard GPR processing flow consisting of dewow filter, gain correction, and elevation correction were applied to these data. Additional processing, in the form of phase-shift migration and Gabor deconvolution was also applied to the data set. The migration algorithm corrected for, among other things, the non-vertical incidence of the GPR raypaths at shallow depths, while the deconvolution accounted for the non-stationary nature of GPR signals throughout the time record. These processing steps greatly improved the quality of the GPR images. Lava tubes were successfully imaged to depths of at least 10 meters using elevated antennas, however, voids smaller than about 2 meters were very difficult to distinguish at any depth.

INTRODUCTION

The Eastern Snake River Plain in southern Idaho, USA is composed in large part of Quaternary basaltic lava flows. Craters of the Moon National Monument is one of several Pleistocene to Holocene lava flows on the Snake River Plain (Kuntz et al., 1986). This field contains more than 60 lava flows erupted from a series of fissure vents known as the Idaho Great Rift. The flows are dated between approximately 15,000 and 2,000 years BP (Kuntz et al., 1986). Though the lava flows at Craters of the Moon bear many features reminiscent of Hawaii-type eruptions, they are distinct from the olivine basalts which make up other flows in the Snake River Plain (Stout et al, 1994). There is some discussion in the scientific community as to whether they can be classified as basalts

* School of Engineering, University of Guelph

(Nicholls, personal communication, 2010). A detailed description of the regional geology can be found in Link et al. (1992).

The focus of this study is the Blue Dragon lava flow, which formed during the most recent eruptive period. Charred vegetation samples from the base of this flow have been radiocarbon dated to an average of 2100 years B.P. (Kuntz et al., 1986). The Blue Dragon is primarily a tube- and surface-fed pahoehoe flow, though it does contain lobes of a'a texture as well (Kuntz et al., 1989). The flow itself covers an estimated area of 280 km², with an estimated volume of 3.4 km³, making it one of the largest flows at Craters of the Moon (Kuntz et al., 1992). Outer edges of the flow reach distances well over 20 km from the vents. The largest flows in this area of the Snake River Plain are consistently fed by systems of lava tubes, indicating the importance of these tubes in insulating and transporting lava over larger distances than would otherwise be possible. (Kuntz et al., 1988, 1992, Harris et al., 2005, Kilburn, 2000, and Cas et al., 1988). Within the Blue Dragon flow, several of these lava tubes are exposed at the surface due to roof collapses, and are a common tourist attraction. The known tube system extends for a distance of several kilometres, and evidence exists for tubes in other, distant areas of the flow (Kuntz et al., 1989a, b). However, it is unclear as to how pervasive these tubes are throughout the flow, or if many of them remain hollow and intact or if they have collapsed or are filled with lava. In addition, even though the flow processes connecting the lava tubes to the vents can be inferred from surface morphologies, relatively little is known about the actual structure of the flow interior.

To gain a better understanding of how the lava tubes interact with the rest of the flow, near-surface (to depths of 10's of meters) geophysical techniques were used to image the sub-surface of the Blue Dragon flow; the method chosen as most suitable was ground penetrating radar (GPR). Previous GPR work has been done at Craters of the Moon by Khan et al. (2007), Heggy et al. (2006) and others. This work focused on imaging the structure of cinder cones and the Great Rift fissure system, as well as differentiating between buried lava flows. In these same studies, the authors also document successful imaging of the roofs of a number of known lava tubes. Outside of Craters of the Moon, GPR has been utilized to image lava tubes by Olhoeft et al. (2000), Miyamoto et al. (2002, 2005), and Meglich et al. (2003), among others. These efforts were generally successful in imaging lava tubes in the near-surface.

The overall purpose of this work at Craters of the Moon is two fold: 1) Build on the success of other works in using GPR to image lava tubes by establishing limits of depth and size of resolvable tubes, and increase the fidelity of the data through higher end processing. 2) Gain insights into the emplacement of the Blue Dragon lava flow, such as the volume and rate of flow supported by lava tubes, and the dominant processes controlling transport and emplacement of lava near the vents. Numerous ground penetrating radar surveys have been performed over the known lava tubes as well as an area nearer to the vents. Figure 1 shows a Google Earth image of the study area, while figure 2 is a photo of the larger of the known lava tubes, Indian Tunnel. This report will focus on understanding the resolution limitations of GPR for imaging lava tubes.

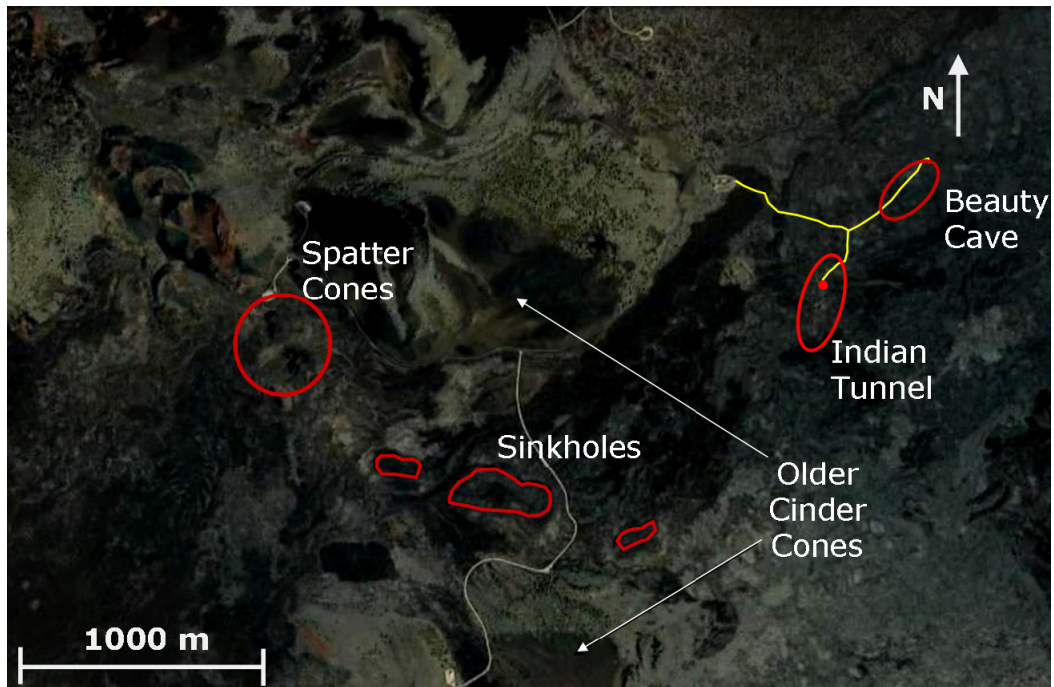


FIG. 1. Annotated satellite image of the Blue Dragon vents and proximal flow. Google Earth™ image.



FIG. 2. Interior of Indian Tunnel lava tube. The tube here is approximately 18 m across and 8 m in height.

GPR THEORY

Ground Penetrating Radar is a geophysical technique used to obtain images of the near-surface. It functions by transmitting electromagnetic energy into the ground, then measuring the amplitude and travel time of waves reflected from boundaries in the subsurface. These boundaries are defined by contrasts in the electrical properties of the ground, the dielectric constant being most significant (Jol, 2009). Large contrasts in dielectric constant will yield larger amplitude reflections, according to equation 1 (assuming vertical incidence):

$$R = \frac{\sqrt{\kappa_1} - \sqrt{\kappa_2}}{\sqrt{\kappa_1} + \sqrt{\kappa_2}} \quad (1)$$

R is the reflection coefficient or relative amplitude of the reflecting wave, and κ_i is the dielectric constant or relative permittivity of medium i (Davis et al., 1989). In addition to reflection amplitudes, the dielectric properties of the Earth also determine the velocity of EM wave propagation. This relation is expressed by

$$v = \frac{c}{\sqrt{\kappa}} \quad (2)$$

where c is the velocity of light in a vacuum, κ is once again the dielectric constant of the medium, and v is the EM velocity in the medium (Jol, 2009). The dielectric constant of air is approximately 1, so from equation 2 it can be seen that EM waves in air will travel very close to a velocity of c . By contrast, the dielectric constant of rocks and earth materials is around 3 to 8, so the EM velocity in the ground drops to around 30-50% of its maximum value (Jol, 2009). GPR typically operates in frequencies between 10 and 1000 MHz. Lower frequencies are able to achieve a greater depth of signal penetration at the cost of resolution. A typical GPR setup consists of a transmitting antenna and receiving antenna in a bi-static configuration, though some systems use a single antenna, or mono-static configuration, to both transmit and receive. Figure 3 shows a simple schematic of a bi-static GPR setup. For a detailed description of GPR theory and applications, see Jol (2009) or Daniels (2004).

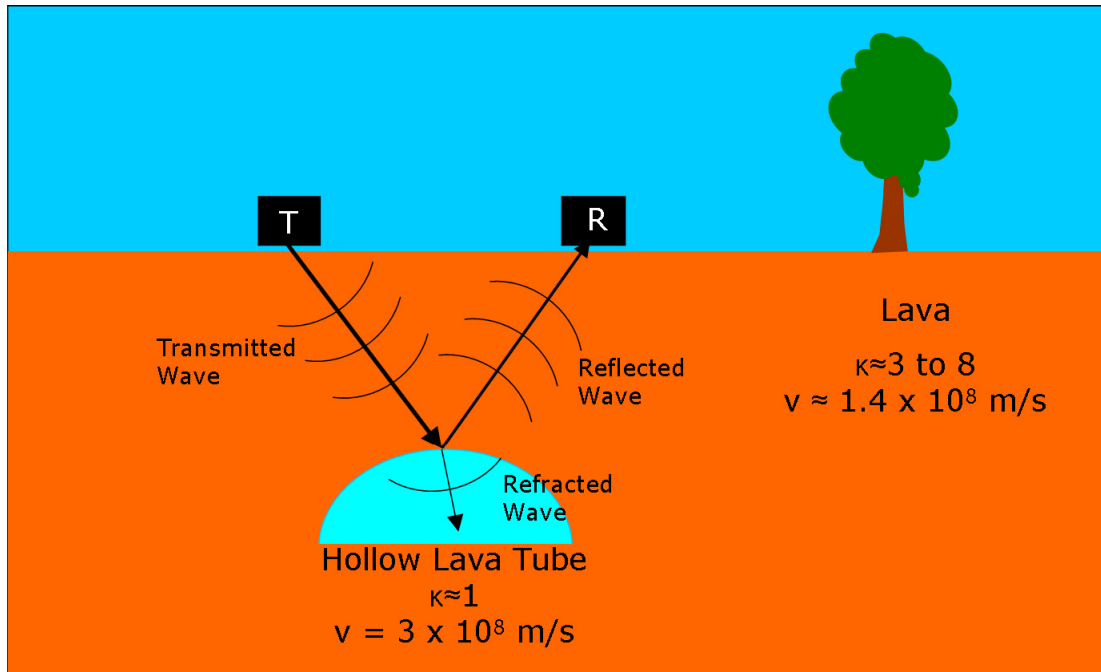


FIG 3. Schematic of GPR reflection survey over a lava flow.

Typical Processing

GPR requires a few standard processing steps to make the data viewable. The initial processing used for the purposes of this research were a dewow filter and gain correction. The ‘wow’ component of GPR data arises from the proximity of the antennas. This proximity causes oversaturation of early signal and inductive coupling between the antennas, which leads to a low-frequency, DC-bias in the data that decays exponentially with time (Jol, 2009). The dewow filter uses a residual mean filter method to calculate a low frequency average for each trace, then subtracts that average to remove the low frequency component and thus remove the bias. Figure 4 shows a GPR trace before and after dewow filtering.

Signals propagating in the earth are subject to a loss of signal amplitude due to effects such as attenuation and geometric spreading. This results in early signal arrivals having much greater amplitude than those arriving later in time (Jol, 2009). The gain correction accounts for this by equalizing the relative amplitudes in each trace to make reflections from later events more visible. The gain correction used for this research was a form of automatic envelope correction. The function, using a given window length, calculates a moving average of the signal for all traces. This produces an average trace envelope, which captures the average decay of the signal amplitudes. The result is then inverted and applied to each trace, which gains signals at latter times.

The above processing steps were compiled in a series of MATLAB scripts by James Irving (1998, unpublished). This set of MATLAB files includes codes to convert GPR data files to MATLAB format, and a number of additional processing and editing scripts. MATLAB was used to perform the majority of processing steps for this project.

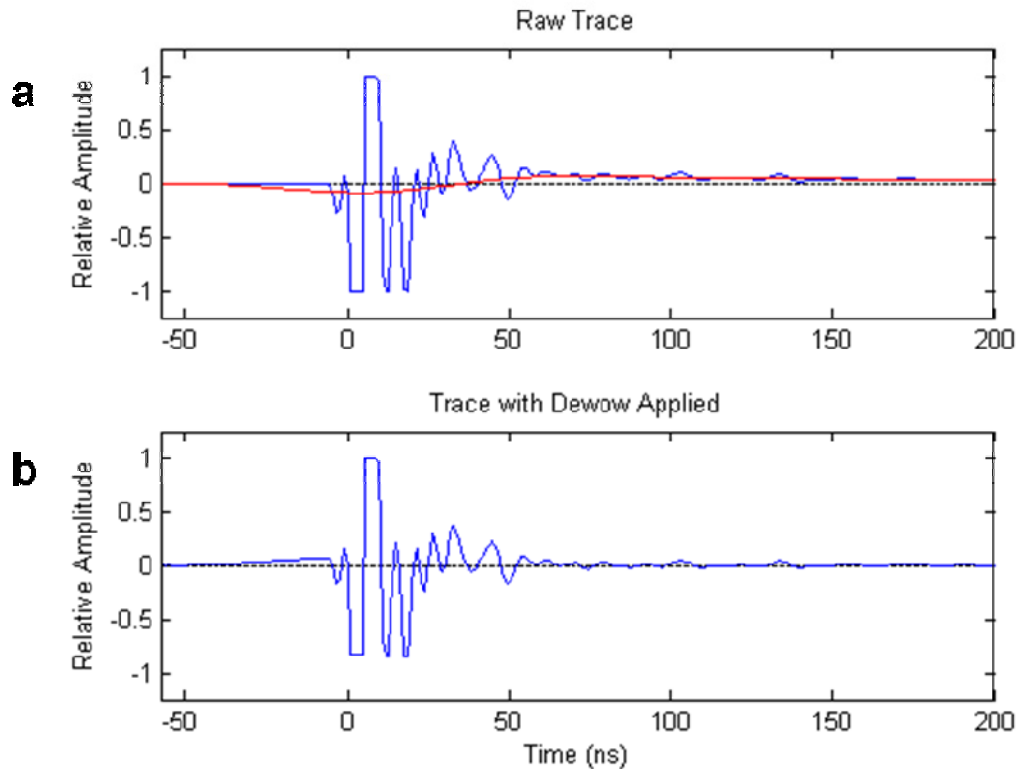


FIG. 4. GPR trace before (a) and after (b) application of dewow filter. The red line in (a) is the wow component which is then subtracted from the raw trace.

Topography Considerations

GPR trace data is recorded from a time-zero position. This means that all traces appear to start from the same elevation in a raw GPR section. However, in areas where elevation varies due to topography, this is obviously not the case. This can result in distortions or apparent variations in structure in the subsurface which do not actually exist. Unless topography is flat, it is therefore necessary to use collected elevation data to apply a static or elevation correction to accurately reflect surface topography in the GPR image. This is done by selecting a datum elevation to act as a zero reference. In this case, the maximum elevation of a line or set of lines was used. The surface elevation of each trace was then subtracted from the datum elevation, and this difference was used to calculate a two-way air travel time for the GPR signal. The trace was then adjusted vertically by this amount.

Migration

Because GPR is, like seismic methods, based upon measuring the travel times of propagating waves, it is subject to some of the same pitfalls associated with seismic methods. Raw seismic and GPR sections do not accurately represent a geologic cross-section. This is because dipping reflectors and point diffractors do not appear in their true spatial positions, because reflected energy is not sent back along the conjugate angle to the angle of incidence. The tool developed for seismic methods to correct these issues

is called migration. Migration is designed to collapse diffractions and dipping reflectors back to their true location and improve spatial resolution, to better reflect the structure of the sub-surface (Yilmaz, 2001). For a more complete description of migration methods, see Yilmaz (2001).

The migration algorithm used in this study is a modified version of Gazdag phase-shift migration (Gazdag, 1978). It applies a 2D pre-stack depth migration (PSDM) individually to each trace, then stacks the traces together to create a migrated section. This allowed the conversion from time-sections to depth-sections, providing a better picture of target depths. For time to depth conversion, using either migration velocity analysis or by converting a raw reflection gather, a velocity model is required. For the work at Craters of the Moon, a constant velocity model was used, since the lava is assumed to be relatively homogeneous. This velocity was determined iteratively through migration velocity analysis (Ferguson et al., 2010). The migration algorithm also accounts for the effects of varying topography, as well as the geometry of GPR surveys (Ferguson et al., 2010). Most seismic migration assumes zero offset between source and receiver, which is a reasonable assumption at greater depths where the reflection angle on a flat layer is close to 90 degrees. In GPR surveys, however, the separation of 1 meter or more between transmitter and receiver results in much lower reflection angles at shallow depth. Thus, the migration algorithm must account for this geometry when calculating the correct position of reflectors (Ferguson et al., 2010).

The migration was applied to ungained GPR sections, since gain functions change relative amplitudes and phase relationships, which should be preserved for accurate migration results (Jol, 2009). After migration, a Gabor domain-based, non-stationary deconvolution was applied to the migrated sections (Margrave et al., 2001 and Margrave et al., 2002). The purpose of deconvolution is to remove the effects of the source wavelet, leaving behind the impulse response of subsurface layers, thereby improving resolution. Seismic deconvolution methods assume a stationary wavelet (i.e. the wavelet frequency content stays constant with time). This is not the case for GPR signals, so stationary algorithms cannot be used. By using a non-stationary deconvolution, deeper events were gained and the overall resolution of the GPR sections was significantly improved. For further detail on the migration and deconvolution applied to this data set, see Ferguson et al. (2010).

IMAGING LAVA TUBES

As mentioned previously, there is significant contrast between the dielectric constant of air and rock. Thus it is expected that a GPR survey will show a high amplitude reflection from the roof and floor of lava tubes and other air-filled voids. This, combined with the relative ease of acquiring GPR data in the field, forms the basis of using GPR as the primary method of imaging lava tubes at the Craters of the Moon site.

To support interpretations of the field data, several forward models were run using a MATLAB program developed by Irving et al., (2006). This script uses a finite-difference, time-domain (FDTD) approach to solve Maxwell's equations in two dimensions for propagating EM waves. A model defining sub-surface dielectric constant, magnetic permeability and electrical conductivity was created as input, which was then

used to simulate the response of a 2D GPR survey. Figure 5a shows a 2D numerical model of dielectric constant for a series of lava tube cross-sections of different size, while figure 5b shows the synthetic output of the forward model.

Prominent diffraction hyperbola can be seen, representing the roof of each tube, followed by a series of reflections marking the floor of the tubes, as well as multiples and more complex reflections, such as those caused by reverberation from tube boundaries. This provides a clear picture of the expected signature of a lava tube in a GPR section, provided the survey is roughly perpendicular to the tube axis.

Field Surveys

Survey 1: Indian Tunnel. This is the largest known lava tube in the vicinity of the Caves Trail. A section of this tunnel approximately 250 m long, between 10 and 20 m wide and approximately 8 m tall is easily accessible to tourists due to several roof collapses along its length. A survey was run along the top of this tunnel between two of the roof collapse holes, or ‘skylights’. This survey consisted of ten 2D lines, spaced from 1 to 2 m apart and approximately 100 m in length. These lines run east-northeast to west-southwest, perpendicular to the tube axis. Figure 6a shows a schematic of the interior of Indian Tunnel, with the approximate locations of the GPR lines on the surface superimposed in red. This tube provides an upper boundary for the size of tube that might be found at Craters of the Moon.

Survey 2: Beauty Cave. This is a smaller segment of the same tube network associated with Indian Tunnel, and is situated northeast of Indian Tunnel as shown in Figure 1. Like Indian Tunnel, Beauty Cave has a number of roof collapses which allow access to the interior. However, at the time of survey the entrances were inaccessible due to the presence of snow and ice. A series of eight 2D lines were surveyed along a length of this cave between two entrances, as shown in figure 6b. The lines were spaced between 10 and 20 meters apart, running NW to SE, again approximately perpendicular to the tube axis. This tube is very useful for the purposes of this study because of its significant variation in size and depth along its profile. With dimensions ranging from several meters across to less than a meter, this tube provides an excellent setting to test the resolution limits of the GPR. Figure 6b is a schematic of the interior of Beauty Cave, again with superimposed GPR lines in red.

Data were acquired in the field using the PulseEKKO Pro GPR system, with a dipole-dipole bi-static antenna configuration. The terrain at the Craters of the Moon site consists of exceptionally rough lava flows, so a simple boom was built to carry the GPR and GPS antenna, to allow for easier navigation and data acquisition. Figure 7 shows a photo of this boom setup in use. Lower frequency antennas were desirable since they would allow greater depth of signal penetration. However, the large size of the lowest frequency antennas made using them over the rough lava impractical. All surveys over known lava tubes were therefore conducted with 100 MHz antennas with antenna spacing of 1 m.

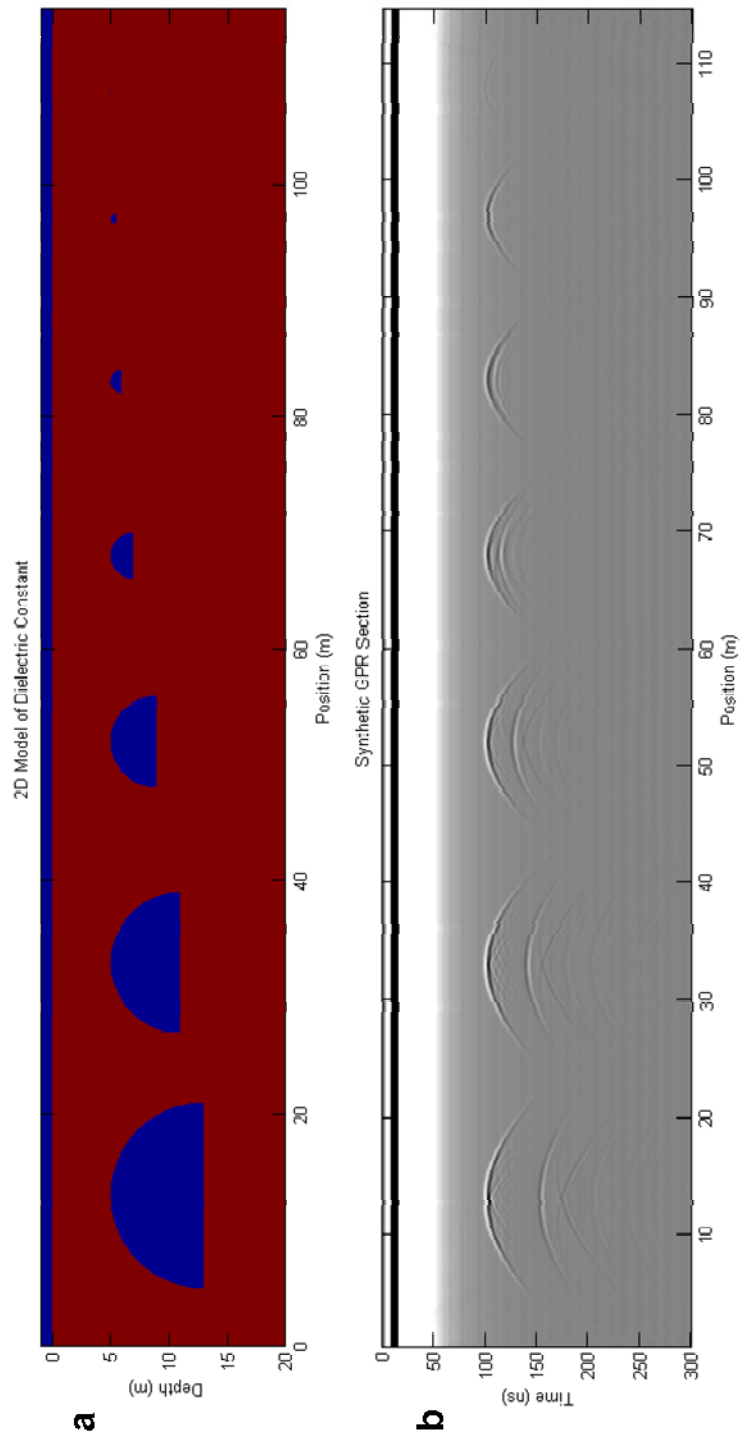
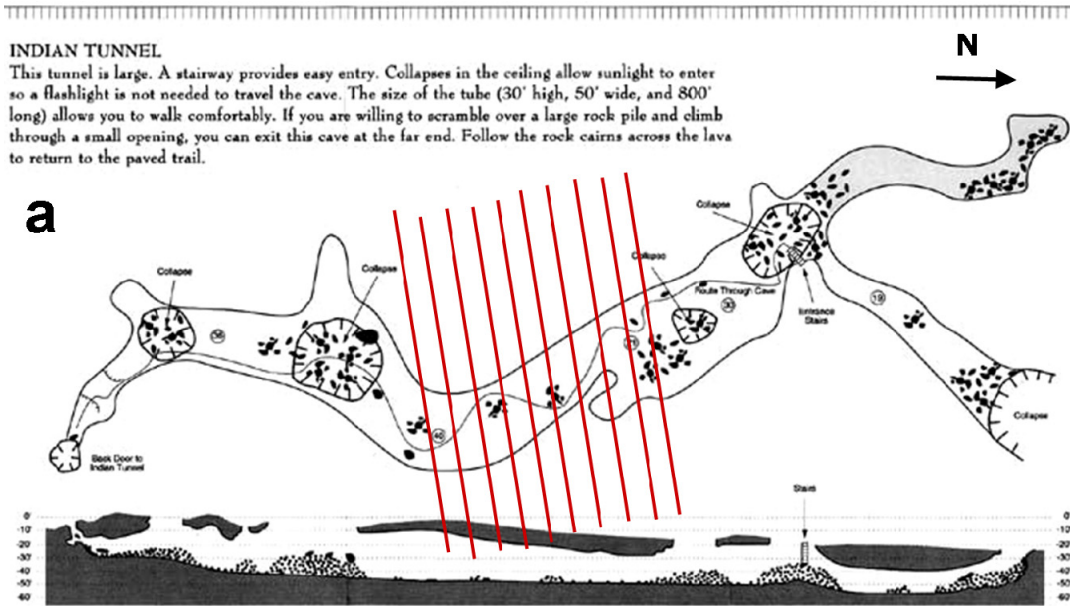
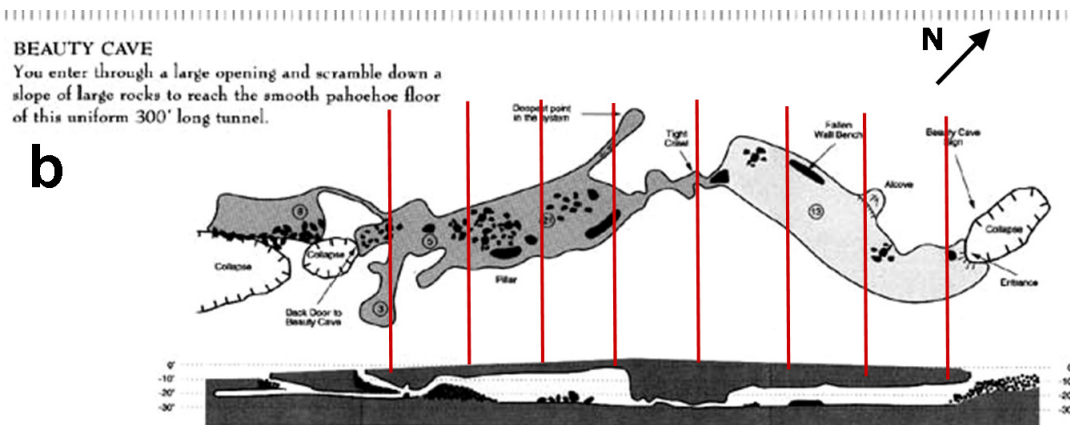


FIG. 5: (a) Dielectric constant model for a series of lava tube cross-sections of decreasing size at constant depth. (b) Synthetic output of the 2D FDTD modelling code.



U.S. National Park Service - www.nps.gov/crmo



U.S. National Park Service - www.nps.gov/crmo

FIG. 6. (a) Schematic of Indian Tunnel, with approximate locations of GPR sections shown in red. (b) Schematic of Beauty Cave, again with approximate GPR sections in red. ((a) and (b) modified from U.S. National Park Service website).

Due to the rough terrain and a need for fast acquisition, GPR lines were acquired by carrying the boom along the line, thus elevating the antennas above the surface by an average of about 20 cm. The GPR was set to fire timed pulses, recording about 3 traces per second. Each trace was sampled at an interval of 0.8 ns, with a time window of 500 ns. Trace positions were recorded with a SOKKIA GSR2700 differential GPS system (attached to top of boom in Figure 7).

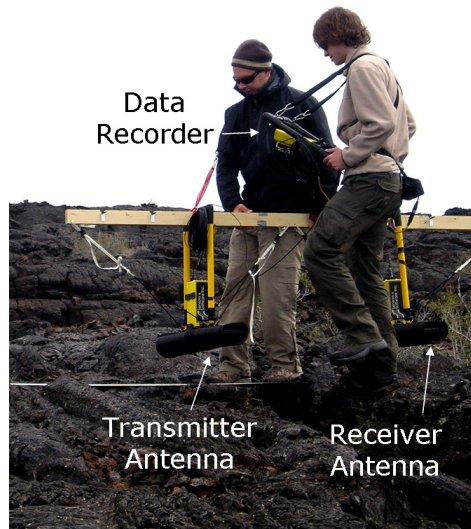


FIG. 7. GPR boom setup as used in the field. The antennas are 100 MHz with a 1 meter separation. Left: James Irving. Right: Colin Rowell. Photo by Erin Ernst.

A challenge that was encountered in the field was the loss of real-time kinematic (RTK) fix between the differential GPS antennas. This often resulted in large, abrupt shifts in the elevation data for some sections of the GPR surveys. MATLAB script was used to convert the PulseEKKO GPS files to MATLAB format. The elevation errors were then corrected by interpolating the between areas in which the RTK was fixed and correct. The corrected elevation data was then used to apply the static shift to the GPR lines. Figure 8 shows one of the acquired sections over Indian Tunnel. The diffraction hyperbola from the tube roof can be seen between 30 and 55 m, from 80 ns at the peak, down to 200 ns at the edges. Note the secondary reflections below, similar to the signature seen in the synthetic model.

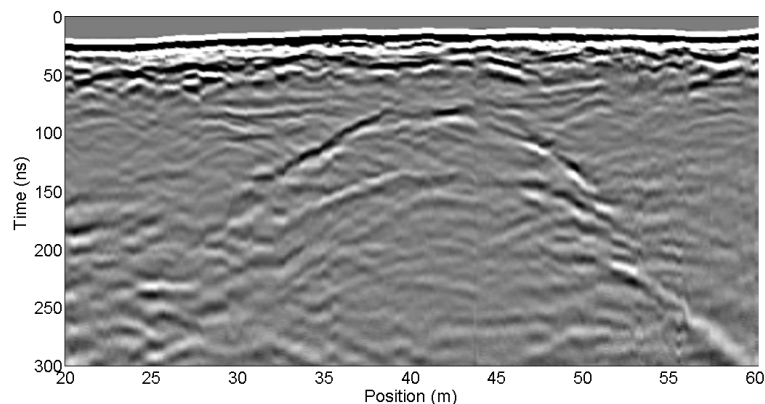


FIG. 8. Piece of a GPR section over Indian Tunnel with dewow, gain, and static correction applied. The diffraction from the roof of the tube is clearly visible. Note the similarity to the synthetic reflection signatures in FIG. 7b.

RESULTS

The image in figure 8 shows one of the higher quality GPR lines over Indian Tunnel, with strong diffractions marking the location of the lava tube. These diffraction patterns can be tracked across adjacent 2D lines to pick the axis of the lava tube. Table 1 shows estimated depths and widths of the two caves for each line, based on the picking of these diffraction hyperbolas.

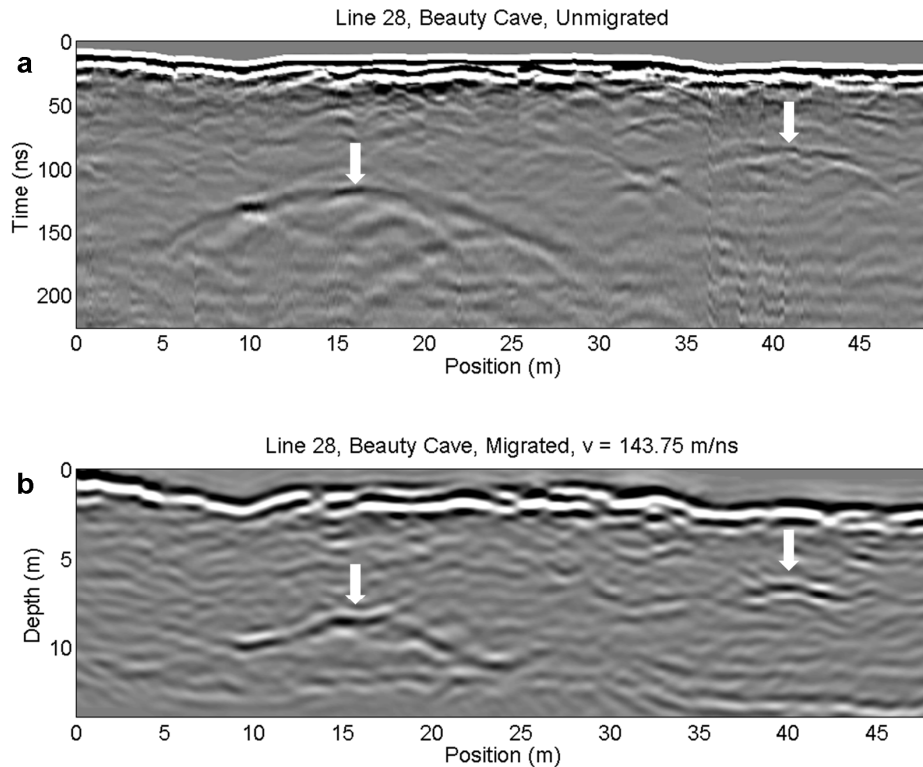


FIG. 9. (a) Unmigrated GPR section over Beauty Cave. The diffraction from the tube roof is centered at a position of about 16 m, and a time of 120 ns. A second diffraction is visible at position 41 m, and at time 80 ns. (b) The same GPR section after migration and deconvolution. The roof reflection has now been collapsed and sharpened, appearing at a depth of about 8 m. The second reflection at 41 m now appears at a depth of about 6 m in the migrated section.

The PSDM algorithm was applied to each line from the Indian Tunnel and Beauty Cave surveys, as well as sections recorded closer to the vents (Ferguson et al, 2010). Figure 9 shows the same section over Beauty Cave before and after migration and deconvolution. This demonstrates vividly the effect of migration in collapsing the diffraction hyperbola from the tube roof to a compact reflection. It also illustrates the improvement in resolution and reduction of noise artifacts. To establish reasonable estimates of the velocity structure, the migration algorithm was used iteratively to narrow the velocity estimates for the area, since a common mid-point survey was not included in the data set. A test line was migrated with several different velocities in an effort to determine the most reasonable velocity. In general, these GPR sections do not penetrate to depths below the base of the Blue Dragon lava flow.

Table 1. Width and depth estimates of tubes from unmigrated and migrated GPR sections.

Unmigrated Sections			Migrated Sections	
GPR Line	Width (m)	Depth (m)	Width (m)	Depth (m)
Indian Tunnel				
15	21.8	1.85	18.1	2.14
16	19.7	3.93	8.9	3.62
17	19.0	4.40	11.6	3.85
18	11.9	4.31	12.2	4.12
19	12.8	3.99	14.0	4.46
20	14.7	3.91	12.9	4.61
21	16.0	3.53	14.2	4.59
22	16.7	3.65	13.1	3.88
23	14.7	4.34	12.9	4.97
24	13.6	3.76	14.2	4.19
Beauty Cave				
28	17.0	6.70	11.7	7.24
29	12.8	5.50	8.9	5.91
30	12.7	5.07	11.9	5.31
31	12.5	10.39	7.3	5.41
32	?	?	?	?
33	13.2	6.94	9.5	8.2
34	13.7	5.14	11.3	6.00
35	10.6	4.22	9.7	4.89

† The tube here is known to narrow abruptly to a small crawl space less than 1 m wide, at depth of 8 to 10 m, but is not visible in the GPR sections.

It is assumed that the sub-surface dielectric properties, and therefore velocity structure, are essentially homogeneous. The obvious exception to this is the presence of void spaces. From these tests, a velocity of 0.143 m/ns was chosen as the mean sub-surface velocity. This value was then used to establish depth axes on the each of the GPR sections, giving reasonable estimates of the depth of signal penetration. Table 1 compares the depth and width estimates from the unmigrated sections to those from the migrated sections. These estimates show that the migration resulted in an increase of depth estimate and a decrease in tube width, in general. The increase in depth is due to an increase in the velocity estimate for the GPR signal. The decrease in tube width is a result of migration collapsing the diffraction hyperbola down to their source locations, allowing the edges of the tube to be picked more reliably.

Interpretation in 3D

The migrated data set consisted of 21 2D GPR sections: 10 over Indian Tunnel, 8 over Beauty Cave, and 3 along the road nearer the volcanic vents. To facilitate the bulk interpretation of the Indian and Beauty surveys, the data were then converted to standard SEG-Y format using MATLAB scripts developed by the Consortium for Research in Elastic Wave Exploration Seismology (CREWES) (Hogan, 2004). This allowed the final processing and interpretations to be performed using 3D visualization software designed for seismic interpretation. VISTA was used to apply bandpass filters to eliminate residual noise, using a low cut of 30 MHz and a high cut of 160 MHz. The filtered and migrated sections were then loaded into the Kingdom Software Suite. This software contains a 3D visualization and interpretation tool called VuPak. The 2D GPR sections could be suspended in 3D space, allowing direct comparison and tracking of tunnel reflectors from section to section. This greatly assists the process of interpreting the often ambiguous reflection patterns. The Kingdom gridding algorithm was then used to interpolate the roof picks between lines using a spline method. The end result was profiles of the tunnel ceilings in 3D. Figure 10a shows the Beauty Cave data set in 3D volume, with the tunnel profile visible connecting the sections. Figures 10b and 10c show the gridded surfaces of Beauty Cave and Indian Tunnel, respectively, with only a single representative GPR section in each.

It is important to note that these interpretations were aided by a-priori knowledge of the tunnel geometries, since their interiors have been explored and mapped. The limits of resolution become more apparent by examining the profile of Beauty Cave in Figure 10b. The sections making up this survey are number 28 through 35. There is a pronounced dip in the roof of Line 32, visible as the blue section of the profile. The tunnel reflector is not distinctly recognizable in this section; however, it is known that this area of the cave narrows abruptly to a crawl space as seen in figure 6b. This section of tunnel, with dimensions only about 1 meter across and 6 to 8 meters deep, is too small and too deep to be resolved by the 100 MHz survey. Only previous knowledge of the cave geometry allowed an estimate pick of the 3D profile.

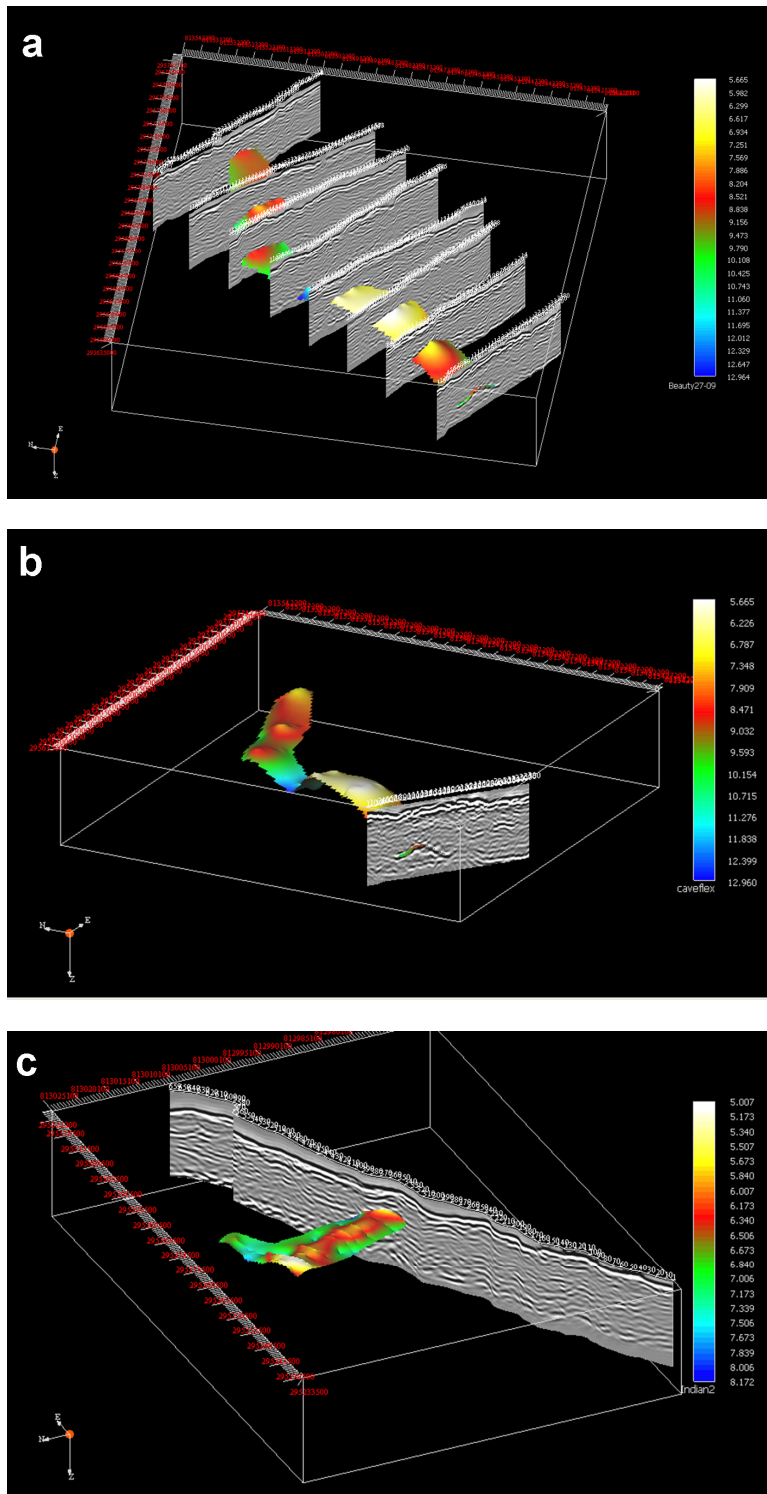


FIG. 10. (a) VuPak image of all Beauty lines and 3D tube profile. Colors indicate depth in m. (b) VuPak image of Beauty Cave profile, showing the same GPR section as FIG. 9 above. (c) VuPak image of Indian Tunnel profile.

CONCLUSIONS

The results of the GPR surveys over Indian Tunnel and Beauty Cave show that GPR is able to resolve lava tubes in the sub-surface at Craters of the Moon. There are limits to the size and depth of resolvable tubes which must be taken into account for the second phase of this study. The main sections of the smaller tube, Beauty Cave, measure between 5 and 10 meters across. These sections were visible to depths of at least 10 meters. The small crawl space in Beauty Cave, at about 1 meter across and 10 meters deep, is beyond the resolution limits of the GPR. It is likely that voids this size would be very difficult to distinguish at any depth. The processing steps of migration and deconvolution produced GPR sections that more closely resembled the actual geometry of the subsurface, as well as improving velocity estimates and depth of imaging. This resulted in greater ability to resolve lava tubes and interpret their geometries than would otherwise have been possible.

In addition to providing a picture of the GPR resolution limits, it has also been shown that good quality data can be collected in this area with the antennas elevated above the surface. The exceptionally rough terrain and need for fast acquisition necessitate carrying the antennas above the surface. While this undoubtedly results in some loss of signal quality, the overall resolution and depth of signal penetration for these surveys are very good.

Ongoing Work

The next phase of this study focuses on the road closer to the volcanic vents. The lava flow here is confined to a valley approximately 1 km wide, defined by two older cinder cones to the North and South. The intent is to search for tube structures within the valley, which would have fed lava from the vents to the tube systems throughout the rest of the flow. The lava flow is much thicker here, and it is very possible that tubes lie as deep as 20 meters or more. In addition, these tubes may be partially filled or collapsed, reducing the probability of obtaining a strong, cohesive reflection in a GPR section. In an effort to obtain a more robust data set, GPR surveys with 50 and 100 MHz antennas in this area have been combined with a micro gravity survey. Though analysis of this data set has yet to be completed, the aim is to correlate reflectors in the GPR sections with lows in the gravity survey, thereby providing a strong indication of void spaces or tubes in the subsurface.

ACKNOWLEDGEMENTS

Special thanks to Dr. Jim Nicholls for providing the motivation and geologic background information for this project. Thanks to Dr. Jim Nicholls, Erin Ernst, Rowan Cockett, and Jakub Topor for assisting with field work, and to Dr. Alastair McClymont for help with field preparation and data analysis. Additional thanks to CREWES for allowing the use of their field equipment to help make this project happen. An NSERC Undergraduate Student Research Award provided funding for the early stage this project. Field work and equipment rentals were paid for through a start-up grant to Dr. Adam Pidlisecky.

REFERENCES

- Cas, R.A.F., Wright, J.V., 1988, *Volcanic Successions Modern and Ancient*: Chapman and Hall.
- Daniels, J.D., 2004, *Ground-Penetrating Radar*, 2nd edition: The Institution of Electrical Engineers.
- Davis, J.L., and Annan, A.P., 1989, Ground-penetrating radar for high-resolution mapping of soil and rock stratigraphy: *Geophysical Prospecting* **37**, 531-551.
- Ferguson, R.J., Pidlisecky, A., and Rowell, C.R., Single-channel PSDM and nonstationary processing of GPR data: CREWES Research Report, **22**, this volume.
- Fernandez, J., and Khan, S., 2005, Identifying sub-surface stratigraphy and source vents with AIRSAR and ground penetrating radar in Craters of the Moon National Monument, Idaho: *SEG Expanded Abstracts*, **24**, 1200.
- Gazdag, J., 1978, Wave equation migration with the phase-shift method: *Geophysics*, **43**, Issue 7, 1342-1351.
- Harris, A., Bailey, J., Calvari, S., and Dehn, J., 2005, Heat loss measured at a lava channel and its implications for down-channel cooling and rheology, *in* Manga, M., and Ventura, G., Eds., *Kinematics and Dynamics of Lava Flows*: Geological Society of America, Special Paper **396**, 125-146.
- Heggy, E., Clifford, S.M., Grimm, R.E., Dinwiddie, C.L., Wyrick, D.Y., and Hill, B.E., 2006, Ground-penetrating radar sounding in mafic lava flows: Assessing attenuation and scattering losses in Mars-analog volcanic terrains: *Journal of Geophysical Research*, **111**, E06S04, 1-16.
- Irving, J., and Knight, R., 2006, Numerical modeling of ground-penetrating radar in 2-D using MATLAB: *Computers and Geosciences*, **32**, Issue 9, 1247-1258.
- Jol, H.M., 2009, *Ground Penetrating Radar: Theory and Applications*: Elsevier Science.
- Khan, S.D., Heggy, E., and Fernandez, J., 2007, Mapping exposed and buried lava flows using synthetic aperture and ground-penetrating radar in Craters of the Moon lava field: *Geophysics*, **72**, No.6, P. B161-B174.
- Kilburn, C.R.J., 2000, Lava flows and flow fields, *in* Sigurdsson, H., Houghton, B.F., McNutt, S.R., Rymer, H., and Stix, J., Eds., *Encyclopaedia of Volcanoes*, Academic Press, 291-306.
- Kuntz, M.A., Spiker, E.C., Rubin, M., Champion, D.E., and Lefebvre, R.H., 1986, Radiocarbon studies of latest pleistocene and Holocene lava flows of the Snake River Plain, Idaho: *Data, Lessons, Interpretations: Quaternary Research*, **25**, 163-176.
- Kuntz, M.A., Covington, H.R., and Schorr, L.J., 1992, An overview of basaltic volcanism of the eastern Snake River Plain, Idaho, *in* Link, P.K., Kuntz, M.A., and Platt, L.B., Eds., *Regional Geology of Eastern Idaho and Western Wyoming*: Geological Society of America, *Memoir* **179**, 227-267.
- Kuntz, M.A., Champion, D.E., Lefebvre, R.H., and Covington, H.R., 1988, Geologic map of the Craters of the Moon, Kings Bowl, and Wapi lava fields, and the Great Rift volcanic rift zone, South-Central Idaho: U.S. Geological Survey Miscellaneous Investigation Series Map I-1632, scale 1:100,000.
- Kuntz, M.A., Lefebvre, R.H., and Champion, D.E., 1989a, Geologic map of the Inferno Cone Quadrangle, Butte County, Idaho: U.S. Geological Survey Miscellaneous Investigation Series Map GQ-1632, scale 1:24,000.

- Kuntz, M.A., Lefebvre, R.H., and Champion, D.E., 1989b, Geologic map of the Watchman Quadrangle, Butte County, Idaho: U.S. Geological Survey Miscellaneous Investigation Series Map GQ-1633, scale 1:24,000.
- Link, P.K., Kuntz, M.A., and Platt, L.B., 1992, Regional geology of eastern Idaho and western Wyoming: Geological Society of America, Memoir 179.
- Margrave, G.F., and Lamoureux, M.P., 2001, Gabor deconvolution: CREWES Research Report, **13**, 18, 241-276.
- Margrave, G.F., Lamoureux, M.P., Grossman, J.P., and Iliescu, V., 2002, Gabor deconvolution of seismic data for source waveform and Q correction: 72nd Ann. Internat. Mtg., Soc. Expl. Geophysc., Expanded Abstracts, 2190-2193.
- Meglich, T.M., Williams, M.C., Hodges, S.M., and DeMarco, M.J., 2003, Subsurface Geophysical Imaging of Lava Tubes, Lava Beds National Monument, CA: Geophysics, December 2003, Orlando, FL.
- Miyamoto, H., Haruyama, J., Rokugawa, S., Onishi, K., and Palmero, A., 2002, Ground penetrating radar to detect lava tubes: preliminary results of a GPR application to Fuji volcano, Japan: Lunar and Planetary Science XXXIII, abstract no. 1482.
- Miyamoto, H., Haruyama, J., Kobayashi, T., Suzuki, K., Okada, T., Nishibori, T., Showman, A.P., Lorenz, R., Mogi, K., Crown, D.A., Rodriguez, J.A.P., Rokugawa, S., Tokunaga, T., and Masumoto, K., 2005, Mapping the structure and depth of lava tubes using ground penetrating radar: Geophysical Research Letters, **32**, 1-5.
- Olhoeft, G.R., Sinex, D.B., Sander, K.A., Lagmanson, M.M., Stillman, D.E., Lewis, S., Clark, B.T., Wallin, E.L., and Kauahikaua, J.P., 2000, Hot and cold lava tube characterization with ground penetrating radar: Eighth International Conference on Ground Penetrating Radar, proceedings vol. **4084**.
- Stout, M.Z., 1975, Mineralogy and petrology of Quaternary lavas, Snake River Plain, Idaho and the cation distribution in natural titanomagnetites: M.Sc. thesis: Calgary, University of Calgary.
- Stout, M.Z., and Nicholls, J., 1977, Mineralogy and petrology of Quaternary lavas from the Snake River Plain, Idaho: Canadian Journal of Earth Sciences, **14**, p. 2140-2156.
- Stout, M.Z., Nicholls, J., and Kuntz, M.A., 1989, Fractionation and contamination processes, Craters of the Moon Lava Field, Idaho, 2000-2500 years BP: Bulletin New Mexico Bureau of Mines & Mineral Resources, **131**, p. 259.
- Stout, M.Z., Nicholls, J., and Kuntz, M.A., 1994, Petrological and mineralogical variations in 2,500-2,000 yr B.P. lava flows, Craters of the Moon Lava Field, Idaho: Journal of Petrology, **35**, p. 1681-1715.
- Yilmaz, O., 2001, Seismic data analysis: processing, inversion, and interpretation of seismic data: Series: Investigations in Geophysics Volume 1, Society of Exploration Geophysicists.